THE JOURNAL OF THE ACOUSTICAL SOCIETY OF KOREA Vol.20, No.3E 2001. 9. pp. 31~37

Analysis of the Cross Talk Mechanism in Capacitive Micromachined Ultrasonic Transducers

Yongrae Rho*, Butrus T. Khuri-Yakub**

*School of Mechanical Engineering, Kyungpook National University
**E. L. Ginzton Laboratory, Stanford University
(Received 7 May 2001; revised 16 Agust 2001; accepted 20 September 2001)

Abstract

Finite element model of a cMUT is constructed using the commercial code ANSYS to analyze the cross talk mechanism. Calculation results of the complex load impedance seen by single capacitor cells are presented, and then followed by a calculation of the plane wave real load impedance seen by a parallel combination of many cells that are used to make a transducer. Cross talk between 1-D array elements is found to be due to two main sources: coupling through a Stoneley wave propagating at the transducer-water interface and coupling through Lamb waves propagating in the substrate. To reduce the cross talk level, the effect of various structural variations of the substrate are investigated, which include a change of its thickness and etched trenches or polymer walls between array elements.

Keywords: *Capacitive micromachined ultrasonic transducer, Cross talk, FEM*

I. Introduction

Capacitor Micromachined Ultrasonic Transducers (cMUT) are gaining acceptance as an alternative to piezoelectric transducers in many applications. They offer the advantage of increased bandwidth with comparable sensitivity to piezoelectric transducers as well as ease of fabrication and electronics integration[1]. The last decade has seen a large increase in the research effort on cMUTs. This is evidenced by the number of research groups throughout the world that are now investigating various aspects of cMUT design, performance, and manufacture[2-5]. Thus far, most of the design and analysis of cMUTs has been done using a simple Mason type equivalent circuit model to predict its behavior[1]. However, the equivalent circuit model lacks some important features such as the coupling into the substrate and the ability to predict cross talk between elements of an array of transducers. Many applications such as ultrasonic imaging, however, demand better understanding and improvement of cMUTs both in terms of individual device performance and array behavior. Considering that cross coupling between elements is one of the most important factors affecting the performance of an array transducer[6], there is a strong need to develop a multi-dimensional analysis technique to identify the sources of the problem and the means to reduce its effect.

In this paper, finite element analyses are performed to investigate the cross coupling mechanism in cMUTs. A two-dimensional finite element model of the cMUT is

Corresponding author: Yongrae Roh (yryong@knu.ac.kr)
Kyungpook National University, Taegu 702-701, Korea

constructed using the commercial code ANSYS©. Through various analyses with the model, we analyze the origin and level of the cross talk between array elements, with evidence of coupling through Stoneley waves propagating at the transducer-water interface and coupling through Lamb waves propagating in the wafer. Further, for the reduction of the cross talk level, the effects of various structural schemes are investigated. These include change of wafer thickness and placement of etched trenches in the wafer to prevent the cross coupling through Lamb waves, as well as placement of acoustic walls between elements to prevent the cross coupling through Stoneley waves.

II. Finite Element Model of a Single cMUT Cell

As a first step to investigate the cross talk mechanism, a single cMUT transducer is modeled with the ANSYS as shown in Figure 1. In the figure we note one transmitter cMUT made of a single capactior cell and two receivers made similarly of single capacitor cell cMUT at the surface of a silicon wafer. The geometry of the three cMUTs is the same. Each consists of a silicon nitride (Si_3N_4) membrane of 0.8 μm thickness and 35 μm diameter and a vacuum gap of 0.15 μm depth in the wafer. This whole solid structure is immersed in water. The transmitter cMUT is excited by a surface pressure distributed over the center half of its membrane surface. The cross talk pressure and displacement are measured in response to the excitation at various points denoted R on the silicon surface, two of which are over the receiver cMUTs, and several over the silicon surface where no cMUTs are placed. Thus, we study the continuing propagation of spurious modes past the cMUTs. The excitation pressure is applied in the form of a square pulse signal of the duration that can cover up to 10 MHz.

Figure 2 is the FE model of the structure in Figure 1. The silicon wafer is chosen to be 4 mm long and 0.5 mm thick. The circumference of the water is enforced by infinite boundary conditions in order to avoid the limit imposed by the finite dimensions in the model. The whole model consists of 26,500 nodes and 26,300 elements. The model is built with the adaptive meshing technique so that high enough accuracy can be maintained in analyzing the micro-motion of the Si_3N_4 membrane with minimal calculation time. Material properties are cited from Ref. 8. The interaction between water and the solid structure is activated by means a specific element type (FLUID29) in ANSYS. With the model, various time domain and frequency domain responses of the structure are obtained through transient and harmonic analyses. Figures 3 and 4 are results of the transient and harmonic analyses, respectively. The calculation step size was 10 nano-second for Figure 3, and 100 Hz for Figure 4, respectively. These responses of the receiver cMUT in relation to the excitation pressure allow the analysis of the cross talk mechanism. The load impedance of each transmitter and receiver cMUT in

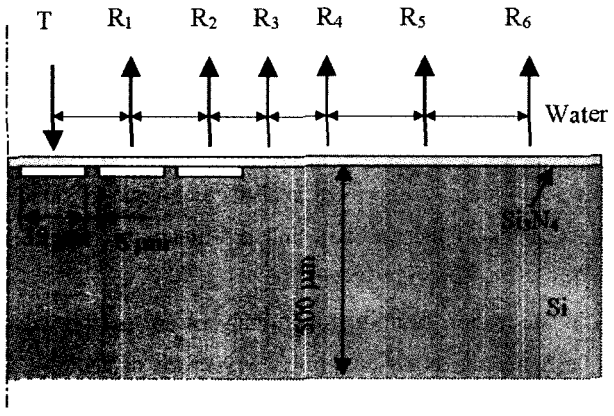

Figure 1. Schematic view of a single cMUT transducer.

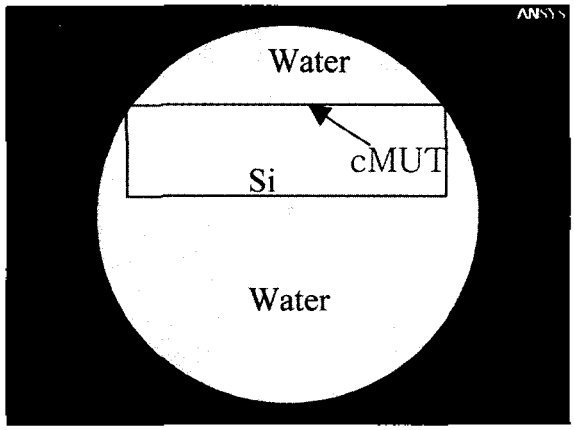

Figure 2. Finite element model of a single cMUT transducer.

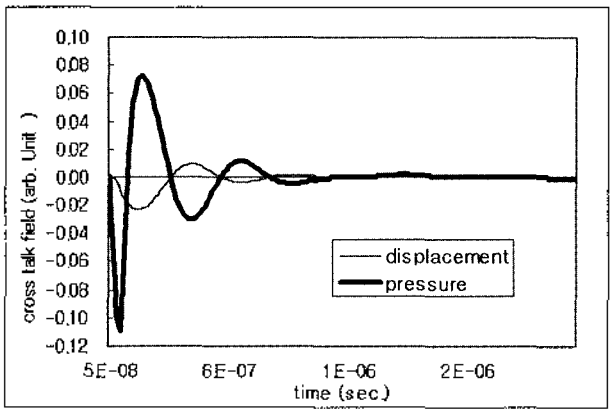

Figure 3. Transient responses of the receiver cMUT, R_1, in Figure 1.

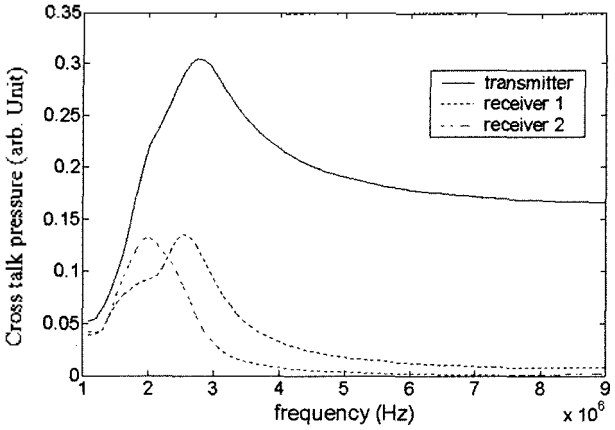

Figure 4. Frequency responses of the three cMUTs, T, R_1 and R_2, in Figure 1.

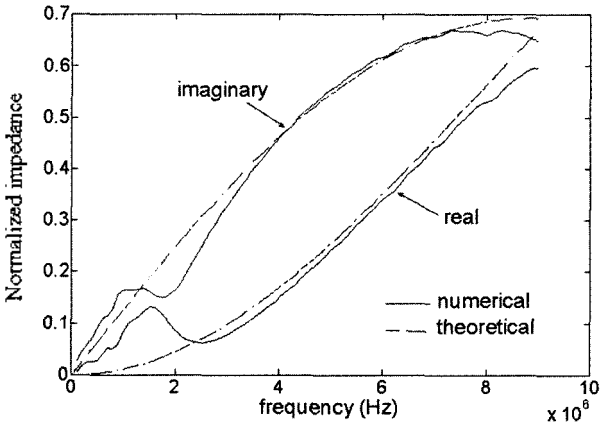

(a) Transmitter cMUT (T)

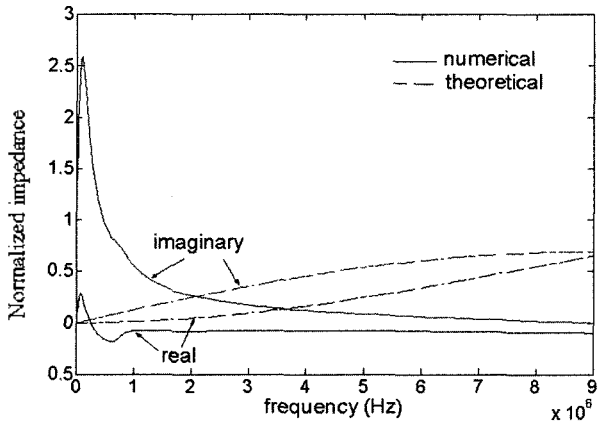

(b) Receiver cMUT (R_1)

Figure 5. Radiation impedance z of a single cMUT cell.

Figure 1 can also be calculated from the frequency spectrum of displacement and pressure. The load impedance z is expressed as Eq. 1 and the results are reported in Figure 5.

$$z = p/i\omega u \tag{1}$$

, where p is acoustic pressure, u is displacement, and ω is the radial excitation frequency. Figure 5-(a) shows that the transmitter cMUT has a complex load impedance (solid line). The complex load impedance means that the transmitter cMUT works almost like a point source due to its small dimension in comparison to the wavelength. The theoretical complex impedance (dotted line) of a circular piston on an infinite baffle is also shown and is compared with the numerical data. The theoretical radiation impedance of a circular piston is expressed as Eq. 2[9].

$$z = \rho c \pi a^2 \left[\left(1 - \frac{2J_1(2ka)}{2ka} \right) - i \left(\frac{2H_1(2ka)}{2ka} \right) \right] \tag{2}$$

, where ρ and c is the density and sound velocity of the radiation medium, respectivcly, J_1 and H_1 is the first order Bessel and Struve function, respectively, k is the wave number, and a is the equivalent radius of the source. The good agreement between the numerical and theoretical values verifies the validity of the finite element model, and proves that there is a direct relationship between the excitation pressure and the excited displacement. On the other hand, in Figure 5-(b), the numerical complex impedance of the receiver cMUT does not show any agreement with the theoretical value, which means that the cross talk pressure has no cause-and-effect relationship with the cross

talk displacement. This result indicates that the cross talk pressure and the displacement at the receiver cMUT are not coupled with each other, and each field has its own means of energy transport. According to the temporal analysis results in Figure 3, the pressure field propagates from the transmitter cMUT to the receiver cMUTs at the speed of the sound velocity in water (1,480 m/s). Therefore, this result and our experimental results reported earlier[7] show that the Stoneley wave propagating along the transducer-water interface is responsible for the cross talk pressure. Similarly, the propagation speed of the displacement field (3,660 m/s) and our previous experimental results[7,10] prove that the fundamental symmetric mode Lamb wave propagating in the Si wafer is responsible for the cross talk membrane displacement.

III. Finite Element Model of a cMUT Array

A finite element model is constructed also for an under-water cMUT array transducer. Figure 6 is the schematic diagram of the array transducer. The geometry and materials of each cMUT in the array are the same as those of the single cMUT cell in Section II. Eight cMUTs are combined in parallel to make either a transmitter array element or a receiver array element. The excitation condition for each cMUT in the transmitter is the same as before. All eight cMUTs in the transmitter array element are excited simultaneously to represent the parallel connection, and

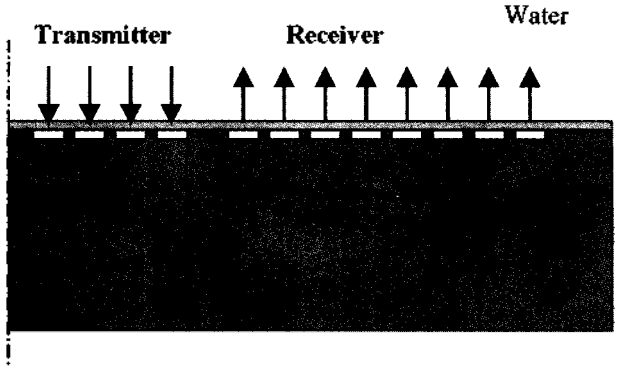

Figure 6. Schematic view of a cMUT array transducer.

the responses of the receiver array element are investigated in relation to the behavior of the transmitter array. The mechanical responses of each cMUT in the receiver array are averaged to simulate their electrical parallel connection. With the model, similar analyses are performed as for the single cell cMUT. The load impedance of the transmitter array is calculated and compared with the theoretical radiation impedance of a circular piston of the same radius on an infinite baffle and presented in Figure 7.

The whole structure of the array is more complicated than the single cMUT, which leads to more discrepancy from the behavior of a pure circular piston. However, in general, the numerical impedance shows a fairly good agreement with the theoretical value, which verifies the validity of the finite element array model, again. The array transducer is composed of eight cMUTs connected in parallel and has much bigger radius than the single cMUT. Hence, the real part of the impedance is more dominant

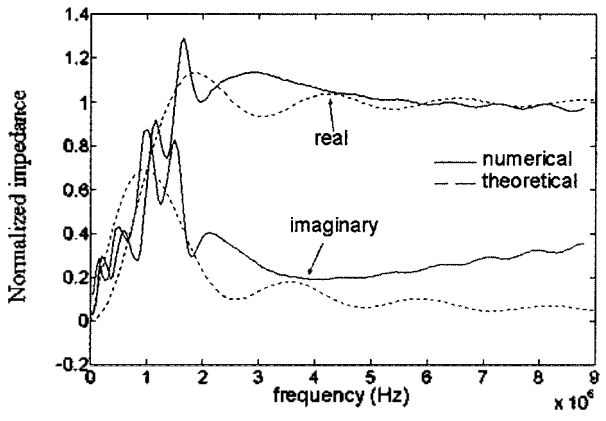

Figure 7. Radiation impedance z of a cMUT array.

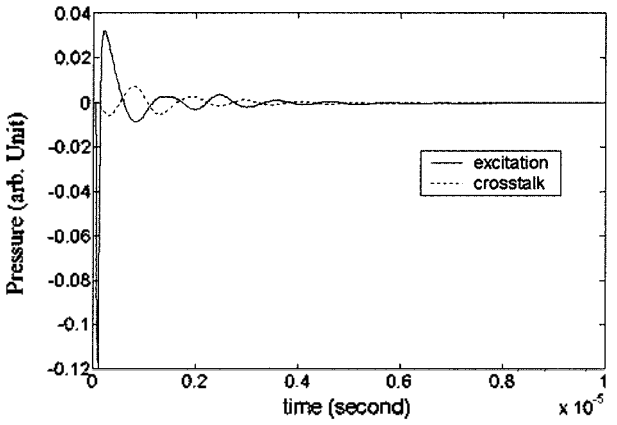

Figure 8. Excitation pressure and cross talk pressure for the cMUT array in Figure 6.

in Figure 7, which means that the array element transducer behaves more like a plane piston than the single cell cMUT. The finite element model also allows us to analyze the transient and harmonic responses of the array transducer. As an illustrative result, Figure 8 is the excitation pressure applied to the transmitter array and the cross talk pressure observed at the receiver array. The figure confirms that cross talk exists between the transmitter array and the receiver array. The level of the cross talk in Figure 8 is -22.6 dB.

IV. Cross Talk Control Structures

Cross coupling between elements is one of the most important factors affecting the performance of an array transducer[2]. Since the cross coupling between array elements has been confirmed through the analyses in Section III, several structural schemes are investigated to reduce the cross talk level. First, we investigate the effect of changing the thickness of the silicon wafer; second, we investigate the effect of placing an etched trench between the array elements; and lastly, we investigate the placement of a wall of a polymer between the array elements. Figure 9 shows the configurations of the trench and the wall. The first two schemes are attempted to reduce the effects of the Lamb wave because the Lamb wave propagates inside the solid wafer, while the third scheme is tried to reduce the effects of the Stoneley wave because most of the Stoneley wave energy resides in the water.

For each of the structural schemes, the same finite element analyses as before are performed to assess the effectiveness of each structure. The influences of these structural variations are shown in Figure 10. Figure 10-(a) is the variation of the cross talk pressure level in relation to the change of wafer thickness. The cross talk level is defined as Eq. 3.

$$\text{Cross talk level} = 20\ Log_{10} | p_{excited} / p_{excitation} | \qquad (3)$$

, where $p_{excitation}$ is the peak pressure excited by the electric pulse signal, and $p_{excited}$ is the peak cross talk pressure induced by the excitation pressure. The cross talk level increases with the thickness of the wafer, although the effect is not very strong. As the wafer is made thicker, the Lamb wave leaks more energy into water due to the change of its velocity that corresponds to the change of its critical angle. According to this result, a thinner wafer is more desirable for cross talk reduction. However, when practical conditions for transducer fabrication are considered, there is a certain limitation in reducing the wafer thickness. Figure 10-(b) shows the variation of the cross talk pressure level in relation to the change of trench depth. In the finite element model, the inside of the trench is set to be vacuum, and the width of the trench is fixed to be 50 μm. In the figure, up to the depth of 200 μm for a 0.5 mm thick wafer, the trench is shown to have almost no effect

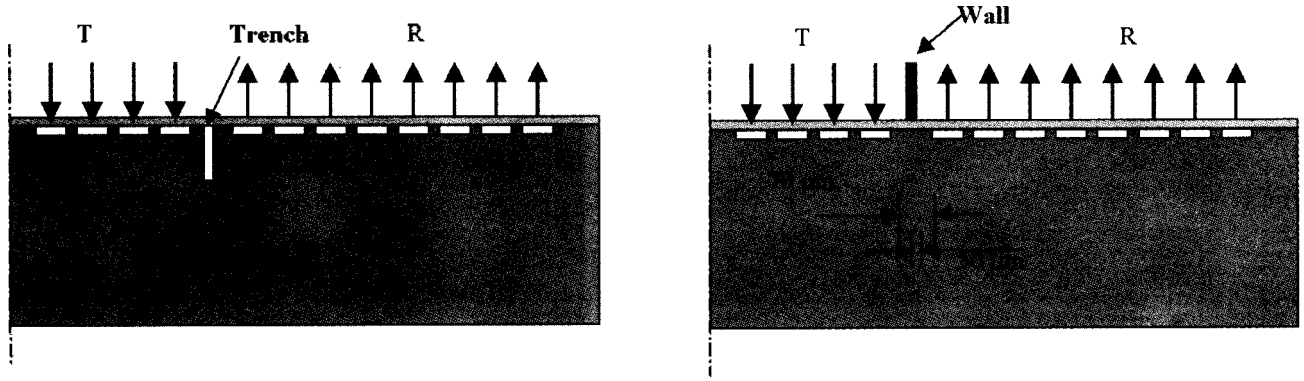

(a) Trench (b) Wall

Figure 9. Schematic view of the cross talk control structures.

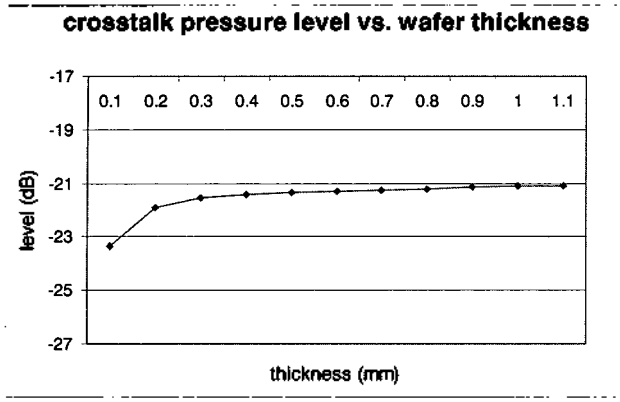

(a) Change of wafer thickness

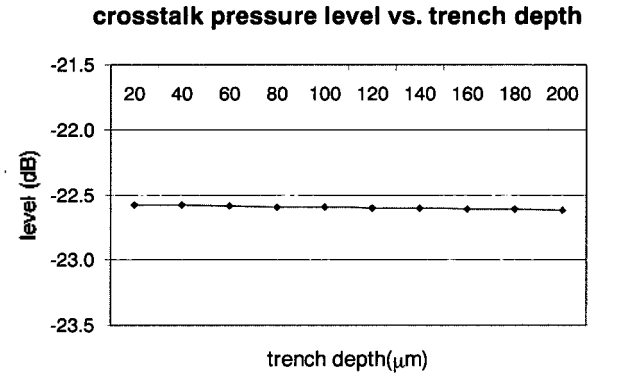

(b) Change of trench depth

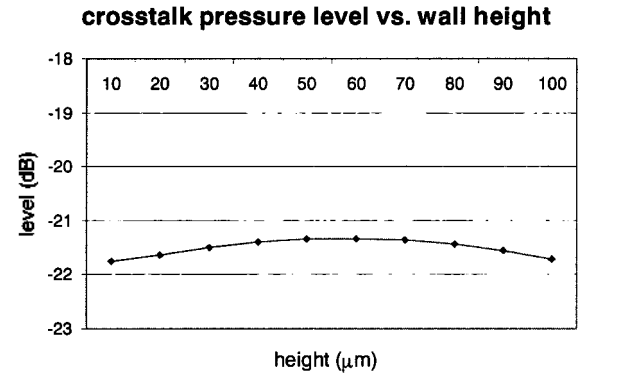

(c) Change of wall height

Figure 10. Effects of cross talk control structures.

in reducing the cross talk level. Since only a portion of the wafer thickness is etched, the Lamb wave propagates as well as without the trench, and thus no reduction in the level. Deeper and wider trenches may help decrease the cross talk level, but they may cause structural weakness of the transducer or change of the transducer radiation pattern. Hence effectiveness of the trenches is not confirmed in this work. Figure 10-(c) shows the variation of the cross talk pressure level in relation to the change of wall height. The wall is made of a common lossy polymer, polyurethane, and the width is fixed to be 50 μm. The wall was placed to perturb the propagation of the Stoneley wave. However, we can observe the cross talk level to increase up to some height of the wall, and then to decreases after that. Careful analysis of the wall motion shows that a higher wall is likely to have its own vibration when the transmitter array is excited and thus generate its own pressure field. The effect of the wall motion results in worse cross talk level as noted in Figure 10-(c). However, with further increase of the height, the role of the acoustic fence to block the wave propagation becomes more prominent, and the resultant cross talk level decreases. Hence, this result says that a well designed wall, such as a wall around each cell, can be an efficient tool to prevent the cross talk between the arrays by the Stoneley wave, but it requires more elaborate design for optimal performance.

V. Conclusion

In this paper, using finite element models of cMUTs, we analyzed the origin and level of cross talk between single cell elements as well as between array elements, with evidence of coupling through Stoneley waves and Lamb waves. The Stoneley wave was found to be responsible for the cross talk pressure field, and the Lamb wave responsible for the cross talk displacement field, respectively. Based on the analyzed mechanism, several structural variations of the silicon wafer were tried to reduce the cross talk level, and their effects were investigated. Of the three structural schemes, placement of a wall between the array elements was found to be the most promising method to control the cross talk, while trenches between the array elements did not show any evidence of cross talk level reduction. Further work will be pursued to elaborate the results in this paper, and that will lead to optimal design of cMUT structures robust to cross talk.

Acknowedgements

This study was supported by a grant of the Korea Health 21 R&D Project, Ministry of Health & Welfare, Republic of Korea (01-PJ1-PG3-31400-0023).

References

1. I. Ladabaum, X. C. Jin, H. T. Soh, A. Atalar, and B. T. Khuri-Yakub, "Surface micromachined capacitive ultrasonic transducers," *IEEE Transactions on Ultrasonics, Ferroelectrics, and Frequency Control*, vol. **45**, no. 3, pp. 678, 1998.
2. K. Suzuki, K. Higuchi, and H. Tanigawa, "A silicon electrostatic ultrasonic transducer," *IEEE Transactions on Ultrasonics, Ferroelectrics, and Frequency Control*, vol. **38**, no. 6, pp. 620, 1998.
3. M. Haller and B. T. Khuri-Yakub, "A surface micromachined electrostatic ultrasonic air transducer," *Proceedings of IEEE Ultrasonics Symposium*, pp. 1241, 1994.
4. D. W. Schindel, D. A. Hutchins, L. Zoou, and M. Sayer, "The design and characterization of micromachined air coupled capacitance transducers," *IEEE Transactions on Ultrasonics, Ferroelectrics, and Frequency Control*, vol. **42**, no. 1, pp. 42, 1995.
5. A. G. Bashford, D. W. Schindel, and D. A. Hutchins, "Micromachined ultrasonic capacitance transducers for immersion applications," *IEEE Transactions on Ultrasonics, Ferroelectrics and Frequency Control*, vol. **45**, no. 2, pp. 367, 1998.
6. J. D. Larson, "Non-ideal radiators in phased array transducers," *Proceedings of IEEE Ultrasonics Symposium*, pp. 673, 1981.
7. X. C. Jin, F. L. Degeretekin, S. Calmes, X. J. Zhang, I. Ladabaum, and B. T. Khuri-Yakub, "Micromachined capacitive transducer arrays for medical ultrasound imaging," *Proceedings of IEEE Ultrasonics Symposium*, pp. 1877, 1998.
8. B. A. Auld, Acoustic fields and waves in solids, 2nd Ed., vol. **1**, Malabar, FL: R. E. Krieger Publishing Co., 1990.
9. A. D. Pierce, Acoustics: an introduction to its physical principles and applications, McGraw-Hill Book Co., 1981.
10. F. L. Degertekin, A. Atalar, and B. T. Khuri-Yakub, "Single mode lamb wave excitation in thin plates by hertzian contacts," Applied Physics Letters, vol. **69**, no. 2, pp. 146, 1996.

[Profile]

• Yongrae Rho

Yongrae Roh received the B.S. and M.S. degrees from Seoul National University in 1984 and 1986, respectively, and the Ph.D. degree from the Pennsylvania State University, U.S.A., in 1990. He worked in the Research Institute of Industrial Science & Technology as a senior research scientist. In 1994, he joined the Kyungpook National University and now is an associate professor in the School of Mechanical Engineering. Major research area is the development of piezoelectric devices and ultrasonic transducers. He has authored more than 100 scientific journal papers, and holds 23 domestic and international patents. He got the Xerox Award, USA, for the best researches in materials in 1990.

• B. T. Khuri-Yakub

B. T. Khuri-Yakub received the Ph.D. degree in 1975 from Stanford University in electrical engineering. He has been a Professor of Electrical Engineering in Stanford University since 1982. His current research interests include in-situ acoustic sensors for monitoring and control of integrated circuits manufacturing processes, micromachining silicon to make acoustic materials and devices such as air borne and water immersion ultrasonic transducers and arrays, and fluid ejectors, and in the field of ultrasonic nondestructive evaluation and acoustic imaging and microscopy.